# Conductive Blends of Thermally Dodecylbenzene Sulfonic Acid-Doped Polyaniline with Thermoplastic Polymers

M. ZILBERMAN,[1] G. I. TITELMAN,[1] A. SIEGMANN,[1] Y. HABA,[2] M. NARKIS,[2] D. ALPERSTEIN[3]

[1] Department of Materials Engineering, Technion—Israel Institute of Technology, Haifa 32000, Israel

[2] Department of Chemical Engineering, Technion—Israel Institute of Technology, Haifa 32000, Israel

[3] Computer Aided Polymer Science Center, P.O. Box 228, Kfar Vradim, Israel

**ABSTRACT:** In the present study, a conductive polyaniline–dodecyl benzene sulfonic acid (PANI–DBSA) complex, prepared by a thermal doping process, and its blends with thermoplastic polymers, prepared by melt processing, were investigated. PANI–DBSA characterization included conductivity measurements, morphology, crystallography, and thermal behavior. The blends' investigation focused on the morphology and the interaction between the components and on the resulting electrical conductivity. The level of interaction between the PANI and the matrix polymer determines the blend morphology and, thus, its electrical conductivity. Similar solubility parameters of the two polymeric components are necessary for a high level of PANI dispersion within the matrix polymer and, thus, enable the formation of conducting paths at low PANI content. The morphology of these blends is described by a two-structure hierarchy: (a) a primary structure, composed of small dispersed polyaniline particles, and (b) a short-range fine fibrillar structure, interconnecting the dispersed particles. © 1997 John Wiley & Sons, Inc. J Appl Polym Sci **66:** 243–253, 1997

**Key words:** polyaniline; thermoplastic polymers; blend; conductivity

## INTRODUCTION

The conventional method for imparting electrical conductivity to common polymers is by admixing conductive solid fillers, such as carbon black or metal particles. The relatively high filler content needed for high electrical conductivity may adversly affect the materials processability and properties. Therefore, there is an increasing interest in processable polymeric materials, using conventional melt-processing techniques, whose electrical conductivity can be tailored for a given application, having attractive mechanical properties. Intrinsically conductive polymers (ICPs), recently making their first utilization appearance, are expected to yield this attractive combination of properties.[1] The presently most common ICPs are polyaniline, polypyrrole, polythiophene, polyacetylene, poly(p-phenylene), and poly(p-phenylene sulfide). Since the backbone of these polymers contains conjugated double donds, they exhibit extraordinary electronic properties, such as low ionization potential and high electron affinity and, as a result, can be easily reduced or oxidized. These polymers undergo "doping" upon exposure to a protonic acid and become electrically conductive.[2] Due to their chain structure and strong intermolecular interactions, undoped ICPs are insoluble in common organic solvents, and melt processing is impossible due to their early decom-

position while still in the solid state. Therefore, they are categorized as intractable, infusible, and difficult to process materials.[2]

Polyaniline (PANI) is presently one of the most promising ICPs. Special interest has been focused on PANI for a number of important reasons: Its conductive form has an excellent chemical stability combined with relatively high levels of electrical conductivity that can be controlled, and the monomer (aniline) is relatively inexpensive and its polymerization is a straightforward, high-yield reaction.[3] Hence, PANI has potential technological applications such as in static films for transparent packaging of electronic components, electromagnetic shielding, rechargable batteries, light-emitting diods, nonlinear optical devices, sensors for medicine and pharmaceutics, and membranes for separation of gas mixtures.[2]

The main disadvantage of conductive PANI, like other ICPs, is its limited thermal processability. One of the methods, still in a development stage, to process PANI, without altering the polymer's structure, is by blending it with conventional polymers. These blends may combine the desired properties of the two components, i.e., the high electrical conductivity of PANI together with the physical and mechanical properties of the matrix polymer. The morphology of such blends has a dominant effect on their properties.

Heeger and co-workers[3–5] reported the use of functionalized protonic acids to both dope emeraldine base (EB, the nonconducting base form of PANI) and, simultaneously, render the resulting PANI complex solubility in common organic solvents. A "functionalized protonic acid" is denoted as $H^+(M^- R)$, where $H^+ M^-$ is a protonic acid group, such as sulfonic acid, and R is an organic group. The proton reacts with the imine nitrogens of PANI, transforming the EB to a conducting salt form. The $(M^- R)$ group serves as a counterion, and the R functional group enhances solubility in common organic solvents and compatibility with conventional polymers; the solubility and compatibility in a given polymer are determined by the structure of the functional group. High-quality conducting polyblends were produced both from solutions containing soluble PANI complexes or by melt blending with various matrix polymers. Recently, the structuring of conductive doped PANI in various matrices by melt processing was described.[6]

The conventional method for doping EB is by mixing it with a functionalized protonic acid in a liquid medium, such as ethanol.[7] Recently, several researchers reported a "thermal doping" process, in which EB and dodecyl benzene sulfonic acid (DBSA) are mixed at a high temperature and the formation of a PANI–DBSA conductive complex occurs. This method enables one to dope PAN and to introduce alkyl substituents to its backbone, without using auxiliary solvents. The presence of unbound, excess DBSA, only physically mixed with PANI, leads to a dispersion of PANI particles in DBSA, a paste which is mainly ionically conducting. Heating causes solidification of the paste, and the PANI–DBSA complex becomes electrically conducting (typically 1–10 S/cm). If large amounts of excess DBSA are used, a plasticized complex is created.[1,8–11]

In most studies of electrically conductive PANI containing polymer blends, blending was performed in a solution, as previously described. Only a few studies concerned with blends prepared by melt processing have been reported.[1,12,13] Shacklette et al.[12] reported that Versicon (Allied-Signal Inc.), a conductive form of PANI, is dispersible in polar thermoplastic matrix polymers such as polycaprolactone and poly(ethylene terephthalate glycol). The percolation threshold for conductivity in these blends was observed in the range of 6–10% v/v of Versicon. Ikkala et al.[1] reported on conductive polymer blends, prepared by blending thermoplastic polymers with Neste Complex (PANI–DBSA prepared by thermal doping), using conventional melt-processing techniques. This research mainly addressed the electrical and mechanical properties of the blends.

In the present study, a conductive PANI–DBSA complex prepared by a thermal doping process and its blends with thermoplastic polymers (prepared by melt processing) were investigated. This research focused on the blends' morphology and the interactions between their polymeric components. These two parameters, which have not been investigated yet for melt-processed blends, have a significant effect on the electrical conductivity. In addition, the characterization of the thermally doped PANI–DBSA complex enables one to better understand its behavior in the blends.

## EXPERIMENTAL

### Materials

#### *Polyaniline (PANI)*

PANI doped with sulfuric acid ($H_2SO_4$) was supplied by Granot (Israel). PANI emeraldine base

(EB) powder was prepared by dedoping the PANI–H₂SO₄ in an aqueous ammonium hydroxide solution, washing with water and acetone, and drying under a vacuum at 40°C. A PANI–DBSA complex was prepared by thermal doping as follows: EB was manually blended with DBSA at a weight ratio of EB : DBSA = 1 : 3, followed by mixing in a Brabender plastograph at 140°C for 5 min. The product was ground into a powder.

### Matrix Polymers

Polystyrene (PS): Galirene HH-102-E (MFI = 4, 200°C, 5 kg), Carmel Olefins, Israel. PS plasticized with dioctyl phthalate (DOP), PS : DOP = 85 : 15. Linear low-density polyethylene (LLDPE): Dowlex NG 5056 (MFI = 1 g/10 min), Dow Chemicals. Copolyamide 6/6.9 (CoPA), a random copolymer of 51% [HN—(CH₂)₅—CO] and 49% [HN—(CH₂)₆—NH—CO—(CH₂)₇—CO] (melt viscosity = 275 Pa-s, 270°C, 122.6 N); EMS, Switzerland.

### Blend Preparation

Binary polymer blends containing a matrix polymer and the PANI–DBSA complex were melt-mixed in a Brabender mixer at 50 rpm for 12 min. The blending temperature varied with the matrix polymer. Blends containing PS or LLDPE were blended at 180°C, and blends containing plasticized PS or CoPA, at 150 and 165°C, respectively. Flat plaques, 3 mm thick, for conductivity measurements were prepared by compression-molding.

### Conductivity Measurements

Electrical conductivity measurements were performed using the "four-probe technique" (ASTM D 991-89) for samples (12 × 1.2 × 0.3 cm³) of conductivity levels > $10^{-7}$ S/cm and the "conductivity measurement between two electrodes" technique (DIN-53596) for the less conductive blends. Samples for the latter technique were first coated with a silver paint to reduce sample–electrode contact resistance. A Keithley 240 A high-voltage supply or a Sorensen Model QRD 60-1,5 was used as power suppliers and a Keithley 614 or 175 electrometer was used as an ampermeter. In addition, a Keithley 610C electrometer was used as a voltmeter for the "four-probe" technique measurements.

### Morphological Characterization

Scanning electron microscopy (SEM) of cryogenically fractured surfaces was performed using a JEOL JSM-840 at an accelerating voltage of 10 kV. The SEM samples were gold-sputtered prior to observation.

### Thermal Analysis

The thermal stability of PANI was investigated by thermogravimetric (TGA) measurements, using a Setaram TG-DTA 92, operated under argon atmosphere at 10°C/min, from 60 to 600°C. PANI's thermal behavior was investigated using an indium calibrated Mettler TC10A differential scanning calorimeter (DSC). Samples of 5 mg were heated at a rate of 10°C from 20 to 500°C, under a N₂ atmosphere.

### X-ray Diffraction

Wide-angle X-ray diffraction was carried out using a Philips PW 1820 X-ray diffractometer and filtered CuKα radiation (λ = 1.54 Å). The diffractometer was operated at 40 kV and 40 mA. The diffraction patterns of PANI powders were obtained by scanning the samples in an interval of $2\theta = 5 \rightarrow 50$ degrees, at a rate of 0.01 degree/s.

### Molecular Simulations

The surface tensions and solubility parameters of the various polymers were evaluated by molecular simulations, using a semiempirical software.[14] The interaction parameters of the matrix polymers with PANI–DBSA were calculated as well. The software principles are described elsewhere.[15]

## RESULTS AND DISCUSSION

### Characterization of the Polyaniline (PANI)

#### Morphology

PANI–H₂SO₄ powder (the original one) consists of chainlike aggregates of fine particles. These "chains," 10–20 μm in length, are composed of a hierarchy of spheres, the smallest being 0.2–0.5 μm in diameter [Fig. 1(a)]. The morphology of the ES is similar to that of PANI–H₂SO₄ [Fig. 1(b)], i.e., the dedoping process does not destroy the fine structure of the as-polymerized material. A similar structure was observed by Shacklette
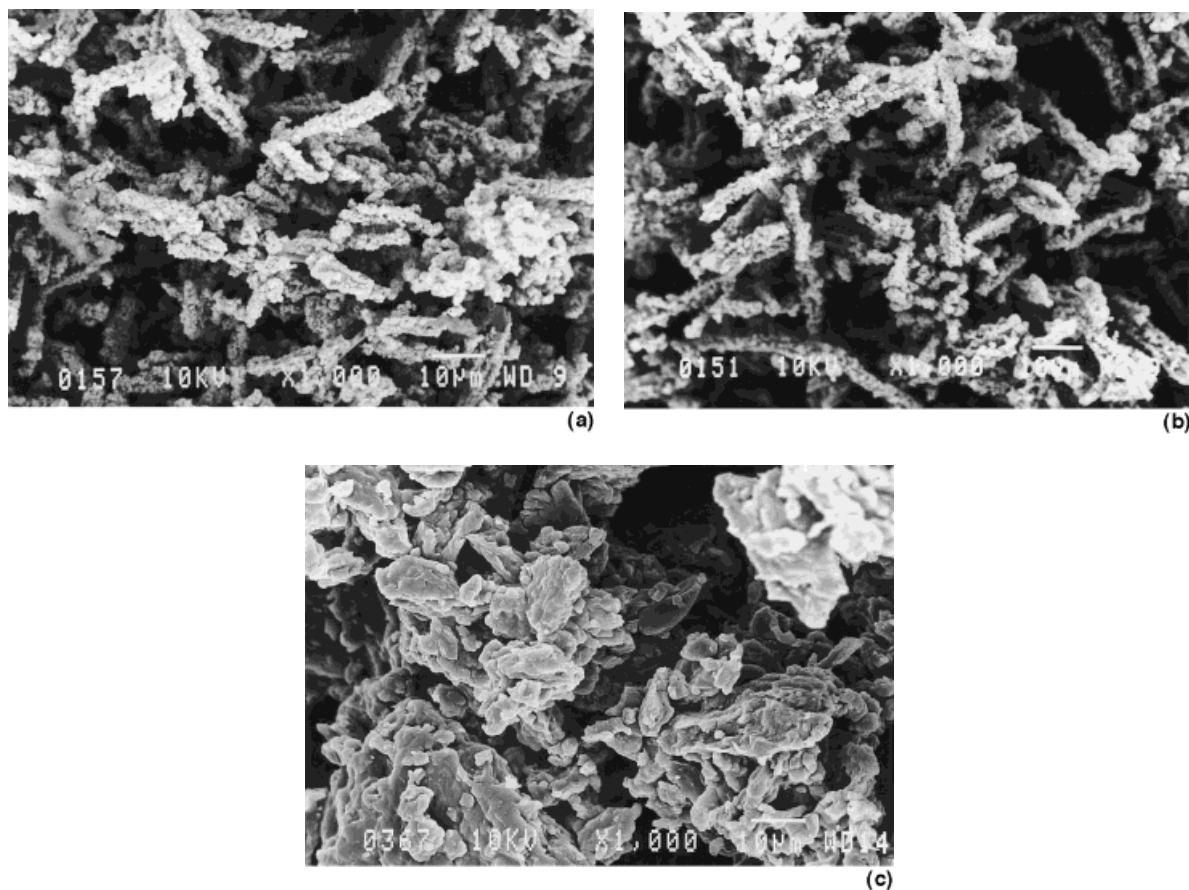
**Figure 1**    SEM micrographs of (a) PANI–H$_2$SO$_4$, (b) EB, and (c) PANI–DBSA.

et al.[12] for Versicon, but with smaller particles (0.05–0.2 $\mu$m).

The morphology of the PANI–DBSA prepared by the thermal doping process is presented in Figure 1(c). Large particles, rather than the original fine structure, are observed due to the combination of intensive mixing, generating stresses and heat during the process of thermal doping in the Brabender mixer.

### Electrical Conductivity and Its Stability

The electrical conductivities of EB, PANI–DBSA, and PANI–H$_2$SO$_4$ are $\sim 10^{-10}$, 1–10, and 0.04 S/cm, respectively, in agreement with the literature.[1,8,10] The thermal redoping with DBSA thus increases the conductivity by about two orders of magnitude. The low electrical conductivity of EB demonstrates the effectiveness of the dedoping process, namely, most of the imine nitrogens of the DBSA-doped PANI are occupied by DBSA and not by H$_2$SO$_4$. It should be mentioned that only 66% of the imine nitrogens in both doped PANIs (i.e., 33% of the total nitrogens) are complexed.

To examine the conductivity thermal stability, PANI–DBSA was exposed to air at elevated temperatures for 1 h. After an exposure to 150°C, the conductivity decreased to 0.3 S/cm and at 200°C to 0.006 S/cm. Wang et al.[16] found that the conductivity of PANI–DBSA and other sulfonic acid-doped PANIs decreases rapidly at temperatures above 200°C. The reasons for this conductivity loss will be discussed later.

### Thermal Analysis

TG thermograms of PANI–DBSA, PANI–H$_2$SO$_4$, and EB are presented in Figure 2. The three thermograms show a small weight loss (2–5%) below 150°C, presumably due to the loss of water and low molecular weight oligomers. The TG thermogram of the EB shows a weight loss onsetting at 440°C, due to polymer decomposition. The doped polymers (PANI–DBSA and PANI–H$_2$SO$_4$) are significantly less thermally stable than are their EB; their weight loss starts at 280°C. Between 280 and 600°C, PANI–DBSA loses 71% of its

weight and PANI–$H_2SO_4$ loses 27% of its weight. Since the two polymers originate from the same EB and their weight losses are almost proportional to their dopant wt %, these weight losses are attributed mainly to a dopant loss (above 440°C, degradation of the polymer also occurs). It should be noticed that the TG thermogram of PANI–DBSA shows a two-step decomposition: A weight loss of 45% occurs at 280–340°C and of 26% above 340°C. Since only 66% of the imine nitrogens of the complex are doped, the PANI : DBSA (1 : 3) contains 25 wt % EB, 28 wt % bound DBSA (acts as a dopant), and 47 wt % excess (free) DBSA. Therefore, it is suggested that the lower-temperature decomposition event is due to the loss of the excess DBSA, and the higher one is due to the loss of the bound DBSA.

DSC thermograms of PANI–DBSA, PANI–$H_2SO_4$, and EB, heated at 10°C/min, are depicted in Figure 3. All thermograms include an endotherm between 20 and 170°C, corresponding to the small weight loss, also of water and oligomers, observed in the TGA. The enthalpy changes of these endotherms (in comparison with the heat of vaporization of water) indicate that the samples include only a small quantity of water (due to the preliminary drying). The EB exhibits a broad, shallow exotherm at 200–400°C, whereas an endotherm at 280°C is observed for PANI–$H_2SO_4$ and at 340°C for PANI–DBSA. The latter exhibits, in addition, a small exotherm at 260°C. The endotherms of the conducting PANIs may stem from the dopant loss, and, indeed, PANI–DBSA shows a double-peak endotherm, which is in agreement with the TGA results. The exotherms
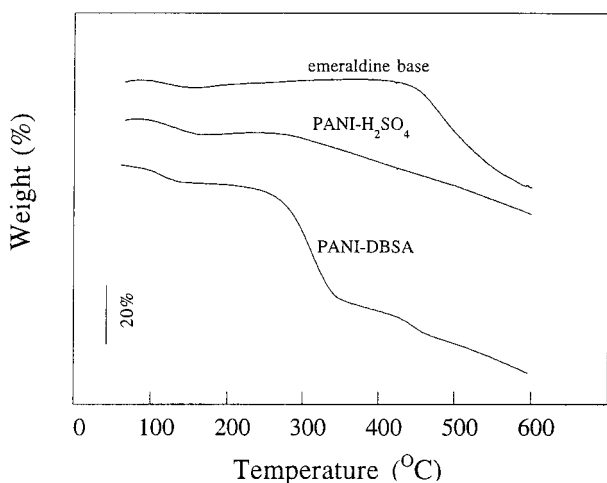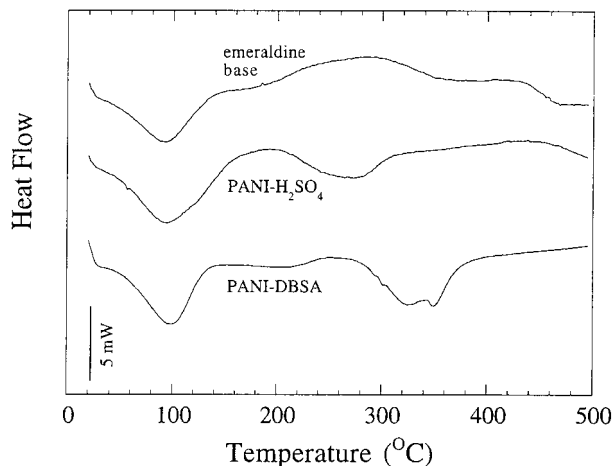


**Figure 3** DSC thermograms of EB and doped PANIs, heated at 10°C/min.

observed for the EB and for PANI–DBSA may stem from changes in the polymers' chain structure, which agree with the conductivity stability results. The irreversible conductivity loss at temperatures below the thermal decomposition temperature indicates that structural rearrangements apparently leading to conjugation loss may be the primary cause for the conductivity loss at 200–280°C. At higher temperatures, thermal degradation is a dominant factor. This conclusion is in agreement with that of Kulkarni and Mathew[17] concerning PANI doped with toluene sulfonic acid. Such changes in the chain structure at high temperatures may be, e.g., crosslinking.[16] The PANI–$H_2SO_4$ is also expected to exhibit an exotherm at 260°C, unobservable due to its overlap with the dopant loss endotherm. It should be mentioned that melting of PANI is not observed in DSC thermograms, due to its early decomposition.

### X-ray Analysis

X-ray diffraction patterns of the PANIs are presented in Figure 4. The EB exhibits three main reflections, at $2\theta = 15°$, 20°, and 25° and a fourth small reflection at $2\theta = 9.5°$. PANI–DBSA and PANI–$H_2SO_4$ exhibit their typical reflections at similar angles. Small deviations are obtained due to different unit cell dimensions, steming from the dopant presence. The structure of the crystalline phases of these PANIs is orthorombic.[18–21] These results agree with those of Fischer et al.[18] and Lux,[19] who observed reflections at the same angles for PANI powders prepared from solutions of concentrated sulfuric acid.



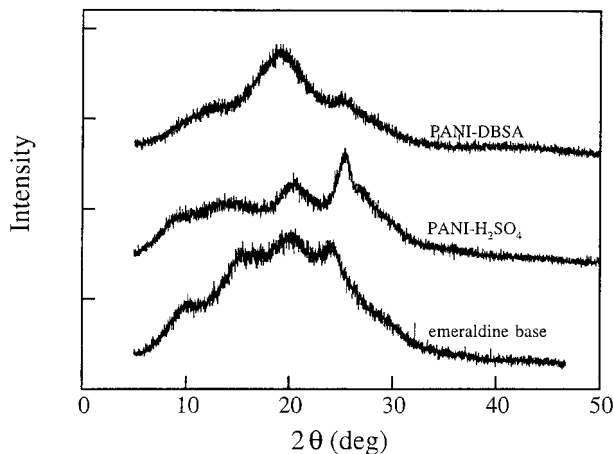**Figure 2** TG thermograms of EB and doped PANIs, heated at 10°C/min.

**Figure 4** X-ray diffraction patterns of EB and doped PANIs.

The degree of crystallinity of these PANIs is relatively low. Since the three polymers exhibit the same amorphous pattern, a comparison of the areas under the curves indicates that the EB is more crystalline than is the doped PANIs. This stems from the presence of bulky dopant molecules in the latter, disturbing crystallization.

## Blends Containing PANI–DBSA and Insulative Thermoplastic Polymers

The electrical conductivity vs. PANI–DBSA content for "melt-blended" PS/PANI–DBSA blends is presented in Figure 5. The percolation threshold occurs at 5 wt % PANI–DBSA, and the PS/ PANI–DBSA (90/10) blend is already conductive ($\sim 10^{-6}$ S/cm), due to the formation of conducting paths of PANI–DBSA within the PS matrix. Beyond percolation, the conductivity level slowly increases with increase in the PANI–DBSA content, due to the generation of a conductive network of an improved quality, attaining $5 \times 10^{-4}$ S/cm for the PS/PANI–DBSA (70/30) blend. It should be emphasized that the actual PANI–DBSA content is smaller than the nominal one (shown in Fig. 5), due to the DBSA excess presence in the thermally doped products. As mentioned above, the 1 : 3 PANI : DBSA blend actually contains 53 wt % PANI–DBSA and 47 wt % free DBSA. Therefore, the effective PANI–DBSA content is about 50% of the nominal (indicated) value. The electrical conductivities of other blends containing 80 wt % matrix polymer and 20 wt % PANI–DBSA are also depicted in Figure 5.

The blends' morphology was studied to eluci-

date the structure responsible for the electrical conductivity behavior. SEM micrographs of cryogenically fractured surfaces of CoPA/PANI–DBSA, LLDPE/PANI–DBSA, and PS/PANI–DBSA blends are presented in Figures 6, 7, and 8, respectively, compared with the morphology of the neat matrix polymers. PANI–DBSA cannot be finely dispersed in CoPA. Moreover, large domains of PANI–DBSA are dispersed within the CoPA matrix [Fig. 6(a)], indicating that continuous networks of PANI–DBSA cannot be formed, resulting in a blend containing 20 wt % PANI–DBSA, which is practically insulative ($\sim 10^{-10}$ S/cm). Smaller particles of PANI–DBSA (0.5–2 $\mu$m) were observed in the LLDPE-based blend [Fig. 7(a)]. The LLDPE/PANI–DBSA (80/20) blend indeed exhibits higher conductivity ($\sim 10^{-8}$ S/cm) than that of the CoPA-based blend. Since DBSA, actually a surfactant, consists of an aromatic ring and a dodecyl aliphatic chain, it enhances the blending and compatibilization of the PANI–DBSA with the aliphatic nonpolar PE rather than with the polar CoPA. Therefore, better conducting networks and smaller particles are generated in the hot-melt blending with the nonpolar aliphatic PE.[6]

The morphology development in the PS/PANI–DBSA blend series is presented in Figure 8. In general, PS [Fig. 8(a)] is brittle and becomes more ductile by the addition of PANI–DBSA [Fig. 8(b)–(d)]. This behavior, not observed in LLDPE and CoPA, may stem from the good dispersibility of some PANI–DBSA within the PS
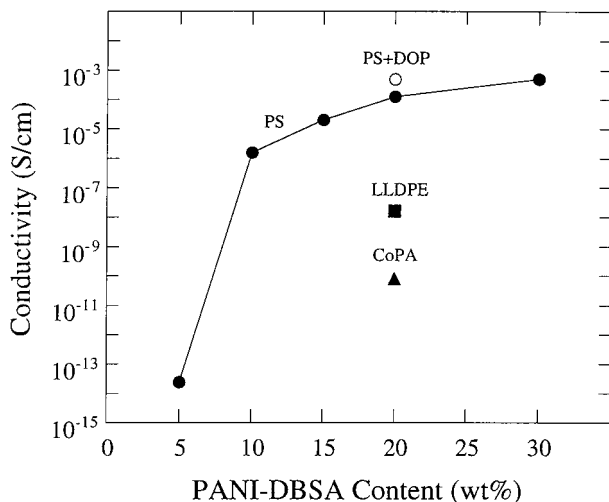


**Figure 5** Electrical conductivity vs. PANI–DBSA content for a PS/PANI–DBSA blend series and for various matrix polymer/PANI–DBSA (80/20) blends.
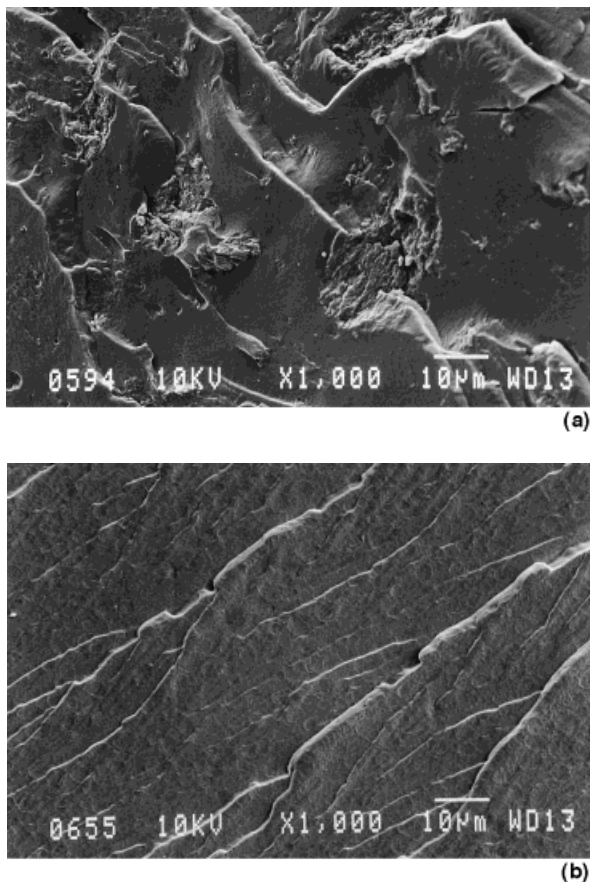
**Figure 6** SEM fractographs of (a) CoPA/PANI–DBSA (80/20) blend and (b) CoPA.

matrix, apparently down to a molecular level. This behavior is attributed to the aromatic nature of PS, consistent with the aromatic EB and the aromatic moiety of the DBSA dopant, as will be discussed later. In addition to the characteristic features of the 90/10 and 80/20 blends' fracture surfaces [Fig. 8(b) and (c)], very small, 0.1–0.2 $\mu$m, PANI–DBSA particles are observed. Therefore, it is suggested that due to the high interaction with the PS matrix the fracturing level of the original PANI–DBSA particles, during melt blending, is relatively high. The 80/20 blend is more ductile than is the 90/10 one, due to the higher excess DBSA content present in the blend. The 70/30 blend [Fig. 8(d)] shows many PANI–DBSA discrete particles at the fracture surface of the sample. These particles are larger than those in the other two blends, presumably due to coalescence of the PANI–DBSA particles. The high conductivity of the PS/PANI–DBSA system at relatively low PANI–DBSA contents is obtained mainly due to the good dispersibility and structur-

ing of the PANI–DBSA particles within the PS matrix.

The level of PANI–DBSA particle fracturing during melt blending depends on the specific matrix used. Both kinetic (viscosities) and thermodynamic (the matrix polymer/PANI–DBSA particles affinity) considerations determine the degree of PANI–DBSA dispersion within the matrix polymer.[22] High interaction levels between the two components enable a higher level of PANI fracturing (at similar matrix viscosity), due to better interphase shear stress transferability.[22] This should occur in systems containing a polymer matrix and PANI–DBSA having similar solubility parameters, i.e., low interaction parameter. Molecular simulations were performed and the calculated surface tensions, solubility parameters, and interaction parameters with PANI–DBSA for the studied polymers are given in Table I. The solubility parameters of DBSA and DOP are presented as well. The thermodynamic parameters predict that the PS-based blends are the
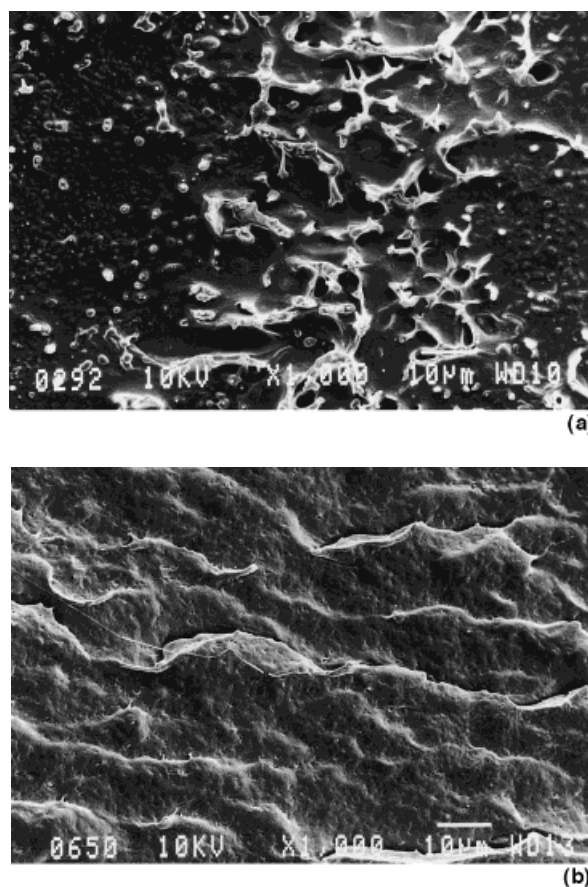




**Figure 7** SEM fractographs of (a) LLDPE/PANI–DBSA (80/20) blend and (b) LLDPE.
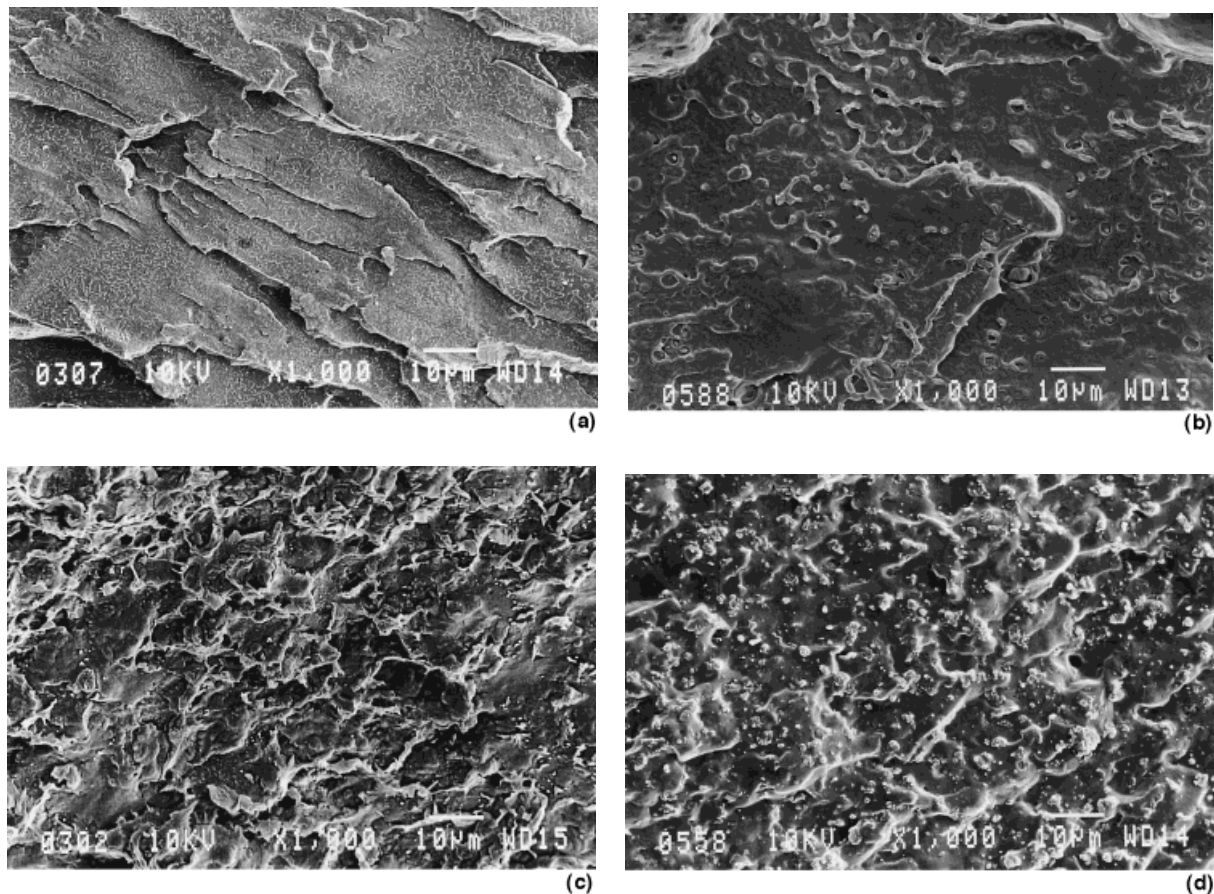
**Figure 8** SEM fractographs of PS/PANI–DBSA blends: (a) 100/0; (b) 90/10; (c) 80/20; (d) 70/30.

most successful systems, while the CoPA-containing blends are the least ones, for obtaining high electrical conductivity. In the former, the similar solubility parameters of the blend's components enable high levels of PANI–DBSA fracturing associated with the formation of conductive paths at relatively low PANI–DBSA contents.

These considerations support the electrical conductivity results (Fig. 5) and morphology observations (Figs. 6–8).

The EB exhibits a solubility parameter of 21.4 $(\mathrm{J/cm^3})^{0.5}$ and a surface tension of 44.4 dyne/cm; both decrease with increase in the DBSA content. Thus, higher degrees of doping will reduce the

**Table I  Calculated Thermodynamic Parameters**

| Polymer | Surface Tension (dyne/cm) | Solubility Parameter $(\mathrm{J/cm^3})^{0.5}$ | Interaction Parameter with PANI–DBSA[a] |
|---|---|---|---|
| PANI–DBSA[a] | 42.7 | 20.8 | |
| EB | 44.4 | 21.4 | |
| PS | 41.0 | 19.5 | 0.07 |
| LLDPE | 35.1 | 16.8 | 0.21 |
| CoPA | 52.5 | 24.2 | 0.79 |
| DBSA | | 18.6 | |
| DOP | | 20.9 | |

[a] Weight ratio of PANI : DBSA = 1 : 1 (excess DBSA was not considered).

PANI–DBSA solubility parameter and surface tension toward those of PS. Similar effects may be predicted and obtained for the LLDPE/PANI–DBSA system. The CoPA matrix exhibits an opposite case since its surface tension and solubility parameter are higher than those of PANI–DBSA, implying that higher degrees of doping will increase the interaction parameter for the CoPA/PANI–DBSA system. The excess DBSA (approximately 47 wt % of the total PANI–DBSA) may be partially dissolved in the PANI and in the PS as well, slightly reducing their solubility parameters. The excess DBSA, $\delta = 18.6 \, (J/cm^3)^{0.5}$, may also influence the LLDPE/PANI–DBSA and CoPA/PANI–DBSA systems. Since the DBSA fraction dissolved in PANI–DBSA, $\delta = 20.8 \, (J/cm^3)^{0.5}$, reduces its solubility parameter, and the fraction dissolved in LLDPE, $\delta = 16.8 \, (J/cm^3)^{0.5}$, increases its solubility parameter, due to the aliphatic part of DBSA, a net reduction effect of the interaction parameter may result. In contrast, since there is a considerable difference between the solubility parameters of DBSA, $\delta = 18.6 \, (J/cm^3)^{0.5}$, and CoPA, $\delta = 24.2 \, (J/cm^3)^{0.5}$, the excess DBSA in the CoPA/PANI–DBSA system will be dispersed mainly in the PANI–DBSA component, decreasing its solubility parameter and, thus, increasing the interaction parameter of this system.

Plasticizing PS by the addition of DOP slightly increases the blends' conductivity (Fig. 5), due to two reasons: (a) The DOP, $\delta = 20.9 \, (J/cm^3)^{0.5}$, increases the solubility parameter of the PS, $\delta = 19.5 \, (J/cm^3)^{0.5}$, toward that of PANI–DBSA, $\delta = 20.8 \, (J/cm^3)^{0.5}$ and, as a result, reduces the interaction parameter of this system. (b) The plasticized matrix enables one to reduce the blending temperature from 180 to 155°C, where the conductivity stability is higher. The first reason has a more prominent effect, since the melt-blending time is relatively short. As previously mentioned, the PANI–DBSA's conductivity stability is sufficient at processing temperatures below 200°C.

The PS conductive blends exhibit very fine PANI–DBSA particles, due to the severe fracturing, but it is still difficult to observe continuous conductive networks which must have been created to impart the measured conductivity. It has thus been suggested, as already pointed out, that a very fine, short-range PANI–DBSA fibrillarlike morphology exists, unobservable by SEM, interconnecting the observable fine dispersed PANI–DBSA particles.[6] Since the solubility parameters of PS and PANI–DBSA are quite similar (Table

I), partial dissolution of PANI–DBSA in the molten PS matrix during blending may occur. Upon cooling, some of the dissolved molecules may remain in solution and some precipitate out, to form a secondary morphology, i.e., a short-range fibrillar structure, interconnecting the dispersed PANI–DBSA fine particles (the primary structure) and thus generating continuous conducting paths. It is assumed that the small quantity of PANI–DBSA molecules remaining dissolved in the matrix does not affect the conductivity. The DOP plasticizer enhances the dissolution of PANI–DBSA in the PS matrix during melt processing, and as a result, a better quality secondary morphology is expected coupled with a higher conductivity.

This research shows that the rules governing the structuring of conductive blends containing PANI are remarkably different from conductive blends containing carbon black.[6] In the latter systems, there are obviously no solubility effects and the structuring occurs during the melt processing/cooling steps, whereas in the former systems in addition to an important particle fracturing process, partial dissolution occurs during the melt processing step, a secondary structure is formed during the cooling step, and the two-structure hierarchy described is more complex.

To further evaluate the advantage of the thermally doped PANI–DBSA, two additional blends were prepared: $[PS + DOP]/PANI–H_2SO_4$ (70/30), and $[PS + DOP]/PANI–DBSA$ (70/30). In the latter, the redoping process was done in ethanol, by a conventional method,[7] rather than by thermal doping. Low electrical conductivities of $2.4 \times 10^{-8}$ and $1.3 \times 10^{-10}$ S/cm, for the $H_2SO_4$ and DBSA dopants, respectively, were measured for these blends, although the doped PANIs exhibit conductivities of 0.04 and 0.15 S/cm, respectively. The PANI–$H_2SO_4$ acts just as a coarse filler, due to its inorganic nature, resulting in a blend of low conductivity even at high PANI–$H_2SO_4$ contents. It should be noticed that the molar PANI–$H_2SO_4$ content in the blend is higher than that of PANI–DBSA; also, the former does not contain any excess dopant. Although the PANI–DBSA doped in ethanol contains a functionalized protonic acid, which is preferred for blending with conventional polymers, its blend with plasticized PS, $[PS + DOP]/PANI–DBSA$ (70/30), is less conductive than is the blend containing thermally doped PANI–DBSA, probably due to the excess DBSA in the latter, which enables better dispersion of the PANI complex in
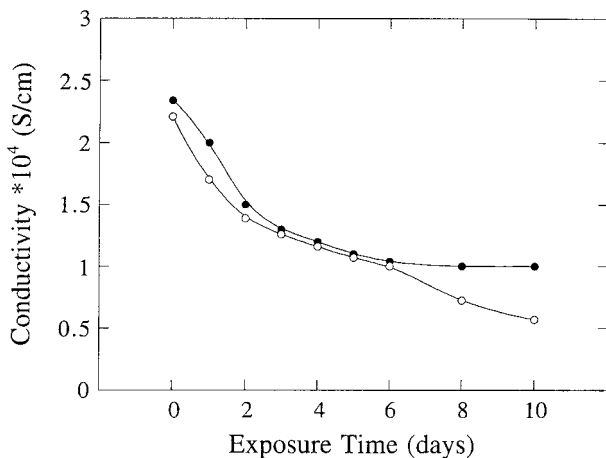
**Figure 9** Electrical conductivity of PS/PANI–DBSA (80/20) blend vs. exposure time at (●) 80°C in vacuum and (○) 50°C in 60% RH.

the matrix polymer. It should be noted that the conventional doping process in ethanol does not enable the existence of excess dopant in the conductive complex, due to the final washing step.

Finally, the stability of the electrical conductivity of the blends at elevated temperatures was investigated. The conductivity of the PS/PANI–DBSA (80/20) blend as a function of exposure time at 80°C in a vacuum and at 50°C in 60% RH are plotted in Figure 9. At 80°C in a vacuum, the conductivity slowly decreases with exposure time and stabilizes after 5 days, while at 50°C in 60% RH, it continues to decrease with time. In both aging conditions, the changes in conductivity are rather small and the blends are thus relatively stable under these conditions.

## SUMMARY AND CONCLUSIONS

PANI–DBSA prepared by thermal doping was blended with several thermoplastic matrices. The PANI–DBSA characterization included conductivity measurements, morphology, crystallography, and thermal behavior. The blends of this PANI–DBSA investigation focused on the morphology and the interaction between the components and on the resulting electrical conductivity.

The thermally doped PANI–DBSA exhibits conductivity levels of 1–10 S/cm. A rapid irreversible conductivity loss occurs above 200°C, due to structural rearrangements leading to loss of conjugation (at 200–280°C) and dopant loss above 280°C. The polymer's backbone decomposes

above 440°C. The PANI–DBSA complex exhibits a coarse morphological structure, due to the intensive mixing of the components in the thermal doping step, which destroys the original aggregates of the EB. An X-ray diffraction pattern indicates a low degree of crystallinity, composed of an orthorombic unit cell.

Both the matrix polymer and the doped PANI type influence the electrical conductivity of the blend, i.e., the level of interaction between the two components determines the PANI–DBSA fracturing and the mode of dispersion within the matrix polymer, the blend's morphology, and, thus, its electrical conductivity.

It has been suggested that the conductive blends exhibit continuous conducting paths, comprising two structures: (a) a primary structure, namely, small dispersed PANI–DBSA particles, and (b) a short-range very fine fibrillar structure, interconnecting the small dispersed particles. The nonconductive blends show large isolated particles within the matrix polymer. Similar solubility parameters of the matrix polymer and the doped PANI are necessary for high-level fracturing of PANI and formation of the conducting paths at low PANI contents.

## REFERENCES

1. O. T. Ikkala, J. Laakso, K. Vakiparta, E. Virtanen, H. Ruohonen, H. Jarvinen, T. Taka, P. Passiniemi, and J. E. Osterholm, *Synth. Met.,* **69,** 97 (1995).
2. J. E. Frommer and R. R. Chance, in *Encyclopedia of Polymer Science and Engineering,* H. F. Mark, Ed., Wiley, New York, 1988, Vol. 5.
3. A. J. Heeger, *Synth. Met.,* **57,** 3471 (1993).
4. Y. Cao, P. Smith, and A. J. Heeger, *Synth. Met.,* **57,** 3514 (1993).
5. C. Y. Yang, Y. Cao, P. Smith, and A. J. Heeger, *Synthetic Metals,* **53,** 293 (1993).
6. M. Narkis, M. Zilberman, and A. Siegmann, *Polym. Adv. Tech.,* to appear.
7. T. J. Laakso and K. Levon, *Solid State Commun.,* **92,** 393 (1994).
8. K. Levon, K. H. Ho, W. Y. Zheng, J. Laakso, T. Karna, T. Taka, and J. E. Osterholm, *Polymer,* **36,** 2733 (1995).
9. O. T. Ikkala, T. M. Lindholm, H. Ruohonen, M. Selantaus, and K. Vakiparta, *Synth. Met.,* **69,** 135 (1995).

10. T. Vikki and O. T. Ikkala, *Synth. Met.,* **69,** 235 (1995).
11. G. Titelman, M. Zilberman, A. Siegmann, Y. Haba, and M. Narkis, to appear.
12. L. W. Shacklette, C. C. Han, and M. H. Luly, *Synth. Met.,* **57,** 3532 (1993).
13. S. J. Davides, T. G. Ryan, C. J. Wilde, and G. Beyer, *Synth. Met.,* **69,** 209 (1995).
14. *Polymer, User Guide,* BIOSYM/MSI, 1995.
15. J. Bicerano, *Prediction of Polymer Principles,* Marcel Dekker, New York, 1993.
16. X. H. Wang, Y. H. Geng, L. X. Wang, X. B. Jing, and F. S. Wang, *Synth. Met.,* **69,** 265 (1995).
17. V. G. Kulkarni and W. R. Mathew, *Synth. Met.,* **41,** 1009 (1991).
18. J. E. Fischer, X. Tan, E. M. Scherr, V. B. Cajipe, and A. G. MacDiarmid, *Synth. Met.,* **41,** 661 (1991).
19. F. Lux, *Polymer,* **35,** 2915 (1994).
20. M. E. Josefowicz, A. J. Epstein, J. P. Pouget, J. G. Masters, A. Ray, Y. Sun, X. Tan, and A. G. MacDiarmid, *Synth. Met.,* **41,** 723 (1991).
21. J. P. Pouget, M. E. Josefowicz, A. J. Epstein, X. Tang, and A. G. MacDiarmid, *Macromolecules,* **24,** 779 (1991).
22. Y. J. Lee, I. Manas-Zloczower, and D. L. Feke, *Polym. Eng. Sci.,* **35,** 1037 (1995).